PHYSICAL REVIEW E, VOLUME 65, 035203(R)

High-dimensional interior crisis in the Kuramoto-Sivashinsky equation

A. C.-L. Chian,[1,2] E. L. Rempel,[1,2] E. E. Macau,[2] R. R. Rosa,[2] and F. Christiansen[3]
[1]*World Institute for Space Environment Research–WISER, NITP, Adelaide University, SA 5005, Australia*
[2]*National Institute for Space Research–INPE, P.O. Box 515, 12227-010 São José dos Campos, SP, Brazil*
[3]*Solar-Terrestrial Physics Division, Danish Meteorological Institute, Lyngbyvej 100, DK-2100 Copenhagen ∅, Denmark*
(Received 13 November 2001; published 13 February 2002)

An investigation of interior crisis of high dimensions in an extended spatiotemporal system exemplified by the Kuramoto-Sivashinsky equation is reported. It is shown that unstable periodic orbits and their associated invariant manifolds in the Poincaré hyperplane can effectively characterize the global bifurcation dynamics of high-dimensional systems.

DOI: 10.1103/PhysRevE.65.035203 PACS number(s): 05.45.Pq, 52.35.Mw, 47.20.Ky

The Kuramoto-Sivashinsky (KS) equation is a widely studied nonlinear reaction-diffusion equation that exhibits a wealth of nonlinear and turbulent states found in spatially extended systems. It was first derived to describe the nonlinear saturation of the collisional trapped-ion mode, a drift wave associated with the oscillation of plasma particles trapped in magnetic wells created by the inhomogeneous magnetic field of a tokamak [1]. This equation is also relevant for other nonlinear plasma phenomena such as the edge-localized-mode in tokamaks [2], glow-discharge structures in near-electrode plasma regions [3], nonlinear coupling of Langmuir and ion-acoustic waves [4], and ionization waves in a neon glow discharge [5], all of which can be modeled by the Ginzburg-Landau-type equation. It has been proved that the KS equation is closely related to the Ginzburg-Landau equation since under certain approximations it governs the phase evolution of the complex amplitude of the Ginzburg-Landau equation [6,7]. In addition to plasma applications, the KS equation can model reaction-diffusion systems in chemical reactions [6], hydrodynamical instability in laminar flame fronts [8], Rayleigh-Bénard convection and flow of a viscous fluid down a vertical plane [9], nonlinear saturation of Rayleigh-Taylor instability in thin films [10], and the dynamics of bright spots formed by self-focusing of a laser beam [11].

Crises are global bifurcations that cause sudden changes in chaotic attractors resulting from the collision of a chaotic attractor with an unstable periodic orbit (UPO) [12]. Interior and boundary crises have been experimentally observed in a CO_2 laser [13], two ions in a Paul trap [14], a magnetoelastic ribbon [15], a pendulum [16], and a leaky-faucet [17]. Recent theoretical studies have indicated that crises can appear in plasmas [18–21]. Intermittency of Alfvén waves in the solar wind plasma can be induced by an interior crisis [18]. Double boundary crises of Alfvén waves are seen in a complex plasma region in the presence of a large number of coexisting attractors [19]. Other types of global bifurcations that lead to crisis and torus breakdown in plasmas have been identified theoretically [20] and experimentally [21].

Most previous analysis of crises are restricted to low-dimensional dynamical systems described by maps or ordinary differential equations [12,18,19]. In this paper, we report interior crisis in an extended, spatiotemporal system described by the KS equation. High-dimensional chaotic dynamical systems may provide a crucial link between low-dimensional chaotic dynamical systems and spatiotemporal chaos (''intermediate'' turbulence) [7]. It was shown that the periodic orbit theory [22] can determine the global averages of the KS equation using the fundamental unstable limit cycles [23]. We argue in this paper that unstable periodic orbits and their associated invariant manifolds in the Poincaré plane can be an effective tool for characterizing high-dimensional global bifurcations in the KS equation, as has been shown in the deterministic dynamical systems of low dimension [12,18,19].

The one-dimensional damped Kuramoto-Sivashinsky equation can be written as [1,6,7,10]

$$\partial_t u = -\partial_x^2 u - \nu \partial_x^4 u - \partial_x u^2, \tag{1}$$

where $u(x,t)$ is subject to periodic boundary conditions $u(x,t)=u(x+2\pi,t)$ and ν is a ''viscosity'' damping parameter. We adopt the spectral method by expanding the solutions in a discrete spatial Fourier series

$$u(x,t)=\sum_{k=-\infty}^{\infty} b_k(t) e^{ikx}. \tag{2}$$

A substitution of Eq. (2) into Eq. (1) yields an infinite set of ordinary differential equations for the complex Fourier coefficients $b_k(t)$,

$$\dot{b}_k(t)=(k^2-\nu k^4)b_k(t)-ik\sum_{m=-\infty}^{\infty} b_m(t)b_{k-m}(t), \tag{3}$$

where the dot denotes derivative with respect to t. Since $u(x,t)$ is a real variable, it follows that $b_{-k}=b_k^*$. We restrict our investigation to the subspace of odd functions $u(x,t)=-u(-x,t)$ and assume that $b_k(t)$ are purely imaginary by setting $b_k(t)=-ia_k(t)/2$, where $a_k(t)$ are real. Under these circumstances, Eq. (3) becomes

$$\dot{a}_k(t)=(k^2-\nu k^4)a_k(t)+\frac{k}{2}\sum_{m=-\infty}^{\infty} a_m(t)a_{k-m}(t), \tag{4}$$

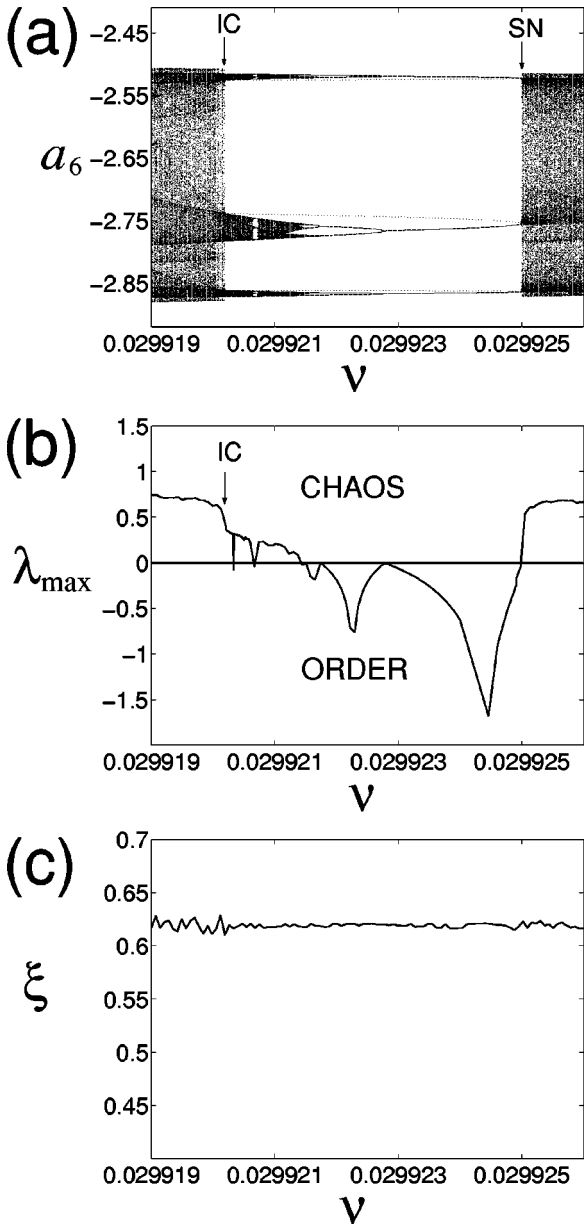

FIG. 1. (a) Bifurcation diagram of a_6 as a function of ν. IC denotes interior crisis and SN denotes saddle-node bifurcation. The dotted lines represent the period-3 unstable periodic orbit. (b) Variation of the maximum Lyapunov exponent λ_{max} with ν. (c) Variation of the correlation length ξ with ν.

where $a_0=0$, $1\leqslant(k,m)\leqslant N$, and N is the truncation order. We solve numerically the high-dimensional dynamical system given by Eq. (4) using a fourth-order variable step Runge-Kutta integration routine. We choose $N=16$, since numerical tests indicate that for the range of the control parameter ν used in this paper the solution dynamics remains essentially unaltered for $N>16$. We adopt a Poincaré map as the $(N-1)$-dimensional hyperplane defined by $a_1=0$, with $\dot{a}_1>0$.

A bifurcation diagram can be obtained from the numerical solutions of the 16-mode truncation of Eq. (4) by varying the control parameter ν. Figure 1(a) shows a period-3 (p-3) window where we plot the Poincaré points of the Fourier component a_6 as a function of ν. The corresponding behavior of the maximum Lyapunov exponent, calculated by the Wolf algorithm [24], is shown in Fig. 1(b). Evidently, the high-dimensional temporal dynamics of the KS equation preserves the typical dynamical features of a low-dimensional dynamical system [12,18,19]. The dotted lines in Fig. 1(a) denote the Poincaré points of the p-3 unstable periodic orbit which emerges via a saddle-node bifurcation at $\nu=0.029\,924\,98$, marked SN in Fig. 1(a). In this paper, we will analyze the role played by this p-3 UPO in the onset of interior crisis at $\nu_{IC}=0.029\,920\,21$, marked IC in Fig. 1.

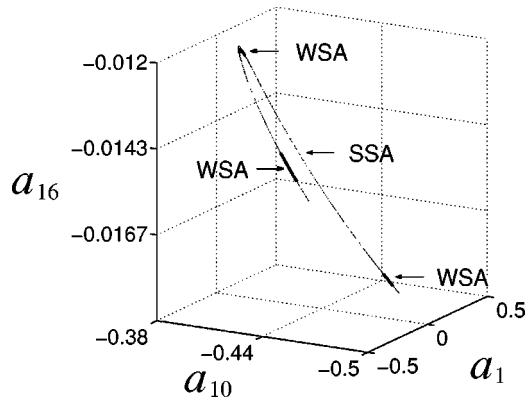

FIG. 2. Three-dimensional projection (a_1,a_{10},a_{16}) of the strong strange attractor SSA (light line) defined in the 15-dimensional Poincaré hyperplane right after crisis at $\nu=0.029\,920\,20$, superimposed by the three-band weak strange attractor WSA (dark line) at crisis ($\nu=0.029\,920\,21$).

The interior crisis at ν_{IC} occurs when the p-3 UPO collides head on with the three-band weak strange attractor evolved from the cascade of period-doubling bifurcations, as seen in Fig. 1(a). The interior crisis leads to a sudden expansion of the strange attractor, turning the weak strange attractor (WSA) into a strong strange attractor (SSA), as seen in Fig. 2. Figure 2 is a three-dimensional projection (a_1,a_{10},a_{16}) of the strong strange attractor (light line) defined in the 15-dimensional Poincaré hyperplane right after crisis ($\nu=0.029\,920\,20$), superimposed by the three-band weak strange attractor (dark line) at crisis ($\nu=0.029\,920\,21$). The interior crisis is characterized by an abrupt jump in the value of the maximum Lyapunov exponent, as indicated in Fig. 1(b). At the crisis point (ν_{IC}) $\lambda_{max}=0.35$, whereas after crisis at $\nu=0.029\,920\,06$, $\lambda_{max}=0.62$. Thus, the interior crisis under consideration results in a sudden increase in the temporal chaoticity of the Kuramoto-Sivashinsky system.

The spatiotemporal pattern of $u(x,t)$ after the interior crisis ($\nu=0.029\,920\,06$) is plotted in Fig. 3. Note that for the chosen value of the damping parameter ν and the spatial system size $L=2\pi$, the dynamics of the Kuramoto-Sivashinsky equation is chaotic in time, but coherent in space [23]. In fact, the spatial coherence remains basically unaltered throughout the whole range of ν used in Fig. 1(a), as indicated by the correlation length ξ [25] in Fig. 1(c).

On the Poincaré hyperplane, an unstable periodic orbit turns into a saddle fixed point, with its associated invariant

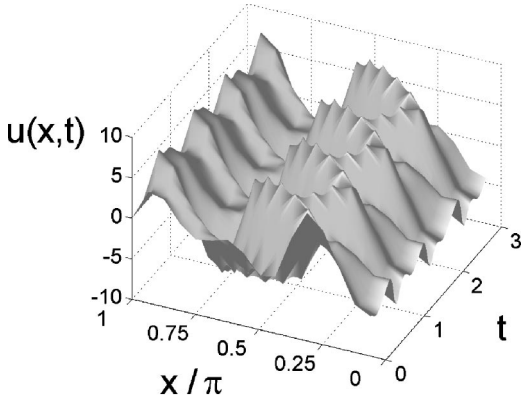

FIG. 3. The spatiotemporal pattern of $u(x,t)$ after crisis at $\nu = 0.029\,920\,06$. The system dynamics is chaotic in time but coherent in space.

stable and unstable manifolds [26]. At crisis ν_{IC} only one of the 16 stability eigenvalues for the p-3 UPO has an absolute value greater than 1, implying that the invariant unstable manifolds are one-dimensional. Of the remaining eigenvalues, one has an absolute value equal to unity and all the other 14 have absolute values less than 1, implying that the invariant stable manifolds have dimension 14. We will focus on the computation of the one-dimensional invariant unstable manifolds since the computation of the invariant stable manifolds of such high dimension is beyond the current state-of-the-art [27]. Figure 4 is a plot of the projection onto three axes (a_1, a_{10}, a_{16}) of the invariant unstable manifolds of the p-3 saddle (denoted by three crosses) right after crisis ($\nu = 0.029\,920\,20$), computed from the You-Kostelich-Yorke (YKY) algorithm [28]. The invariant unstable manifolds consist of infinitely many distinct, discrete Poincaré points whose backward orbits converge to the saddle [26].

We proceed next with the characterization of the high-dimensional crisis at ν_{IC} by showing in Fig. 5 the collision of the weak strange attractor with the p-3 UPO in the reduced two-dimensional Poincaré plane (a_5 versus a_6), in the vicinity of the upper fixed point in Fig. 4. The dark line denotes the strange attractor, and the light line denotes the numerically computed invariant unstable manifolds of the saddle.

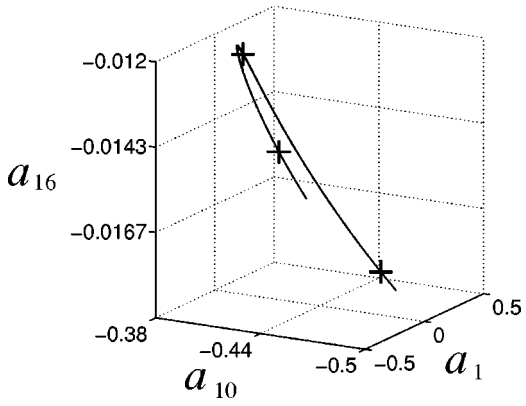

FIG. 4. Three-dimensional projection (a_1, a_{10}, a_{16}) of the invariant unstable manifolds of the period-3 saddle (crosses) right after crisis at $\nu = 0.029\,920\,20$.

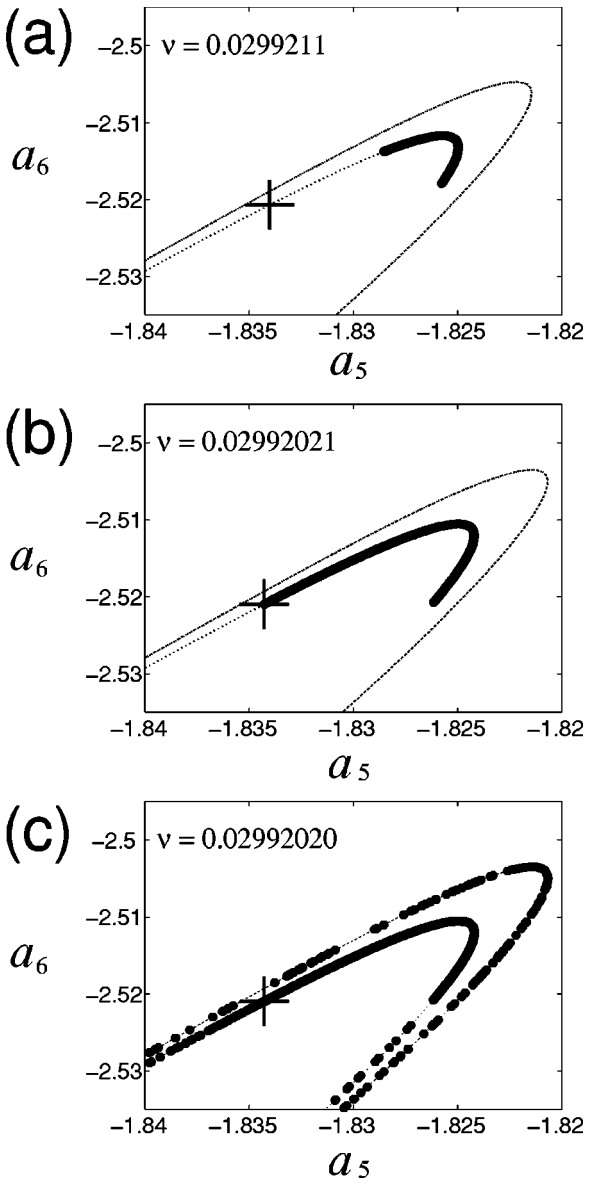

FIG. 5. The plots of the strange attractor (dark line) and invariant unstable manifolds (light lines) of the saddle before (a), at (b), and after (c) crisis. The cross denotes one of the saddle points.

Figures 5(a)–5(c) display the dynamics before, at, and after crisis, respectively. Note that the strange attractor always ''overlaps'' the invariant unstable manifolds. Figure 5(b) shows the ''head-on'' collision of the weak strange attractor with the p-3 UPO at ν_{IC}, which proves the occurrence of an interior crisis [12,19,26]. This collision leads to an abrupt expansion of the strange attractor and a sudden increase in the system chaoticity, as seen in Fig. 5(c). A comparison of Figs. 2 and 4 confirms that, after crisis, the strong strange attractor and the invariant unstable manifolds ''overlap'' with each other.

In conclusion, we have shown that high-dimensional interior crisis can be found in spatially extended systems exemplified by the Kuramoto-Sivashinsky equation. Although we have adopted a 16-mode truncated system in our analysis, all

the calculations performed can be extended to an arbitrary high number ($N<\infty$) of modes for an appropriate choice of ν and L. The identification of the unstable periodic orbits and their invariant manifolds is fundamental for monitoring and controlling the instabilities, chaos, and turbulence in tokamak experiments [29]. Further theoretical and experimental studies of high-dimensional dynamical systems, following the methodology developed in this paper, may improve confinement in tokamaks and the understanding of other complex systems.

This work is supported by CNPq, FAPESP, and AFOSR. A.C.-L.C and E.L.R. wish to thank Professor A. W. Thomas and Professor A. G. Williams of Adelaide University for their kind hospitality.

[1] R.E. LaQuey *et al.*, Phys. Rev. Lett. **34**, 391 (1975); B.I. Cohen *et al.*, Nucl. Fusion **16**, 971 (1976).
[2] S.I. Itoh *et al.*, Phys. Rev. Lett. **67**, 2485 (1991); S.I. Itoh, K. Itoh, and A. Fukuyama, Nucl. Fusion **33**, 1445 (1993).
[3] M.S. Benilov, Phys. Rev. A **45**, 5901 (1992).
[4] R. Erichsen, L.G. Brunnet, and F.B. Rizzato, Phys. Rev. E **60**, 6566 (1999).
[5] B. Bruhn and B.P. Koch, Phys. Rev. E **61**, 3078 (2000); B. Bruhn *et al.*, Phys. Plasmas **8**, 146 (2001).
[6] Y. Kuramoto and T. Tsuzuki, Prog. Theor. Phys. **55**, 356 (1976).
[7] P. Manneville, *Dissipative Structures and Weak Turbulence* (Academic Press, San Diego, 1990); T. Bohr *et al.*, *Dynamical Systems Approach to Turbulence* (Cambridge University Press, Cambridge, 1998).
[8] G.I. Sivashinsky, Acta Astron. **4**, 1177 (1977).
[9] G.I. Sivashinsky and D.M. Michelson, Prog. Theor. Phys. **63**, 2112 (1980).
[10] A.J. Babchin *et al.*, Phys. Fluids **26**, 3159 (1983).
[11] M. Münkel and F. Kaiser, Physica D **98**, 156 (1996).
[12] C. Grebogi, E. Ott, and J.A. Yorke, Phys. Rev. Lett. **48**, 1507 (1982); Physica D **7**, 181 (1983); C. Grebogi *et al.*, Phys. Rev. A **36**, 5365 (1987); K.G. Szabó *et al.*, Phys. Rev. E **61**, 5019 (2000); C. Robert *et al.*, Physica D **144**, 44 (2000).
[13] D. Dangoisse, P. Glorieux, and D. Hennequin, Phys. Rev. Lett. **57**, 2657 (1986).
[14] J.A. Hoffnagle *et al.*, Phys. Rev. Lett. **61**, 255 (1988).
[15] W.L. Ditto *et al.*, Phys. Rev. Lett. **63**, 923 (1989).
[16] R.W. Leven and M. Selent, Chaos, Solitons Fractals **4**, 2217 (1994).
[17] J.C. Sartorelli, W.M. Gonçalves, and R.D. Pinto, Phys. Rev. E **49**, 3963 (1994); R.D. Pinto and J.C. Sartorelli, *ibid.* **61**, 342 (2000).
[18] A.C.-L. Chian, F.A. Borotto, and W.D. Gonzalez, Astrophys. J. **505**, 993 (1998).
[19] A. C.-L. Chian, F. A. Borotto, and E. L. Rempel, Int. J. Bifurcation Chaos (to be published).
[20] Kaifen He, Phys. Rev. Lett. **80**, 696 (1998); Phys. Rev. E **59**, 5278 (1999); Phys. Rev. Lett. **84**, 3290 (2000); Phys. Rev. E **63**, 016218 (2001).
[21] C. Letellier *et al.*, Phys. Rev. E **63**, 042702 (2001).
[22] P. Cvitanović, Phys. Rev. Lett. **61**, 2729 (1988); R. Artuso, E. Aurell, and P. Cvitanović, Nonlinearity **3**, 325 (1990).
[23] F. Christiansen, P. Cvitanović, and V. Putkaradze, Nonlinearity **10**, 55 (1997).
[24] A. Wolf *et al.*, Physica D **16**, 285 (1985).
[25] S.W. Morris *et al.*, Phys. Rev. Lett. **71**, 2026 (1993).
[26] K. T. Alligood, T. D. Sauer, and J. A. Yorke, *Chaos: An Introduction to Dynamical Systems* (Springer-Verlag, New York, 1996).
[27] M.E. Johnson, M.S. Jolly, and I.G. Kevrekidis, Int. J. Bifurcation Chaos Appl. Sci. Eng. **11**, 1 (2001).
[28] Z. You, E.J. Kostelich, and J.A. Yorke, Int. J. Bifurcation Chaos Appl. Sci. Eng. **1**, 605 (1991).
[29] P.E. Bak *et al.*, Phys. Rev. Lett. **83**, 1339 (1999); P.E. Bak, and R. Yoshiro, Contrib. Plasma Phys. **40**, 227 (2000).